RESEARCH ARTICLE

WILEY

Subcellular localization of the enterobacterial common antigen GT-E-like glycosyltransferase, WecG

Nicholas Maczuga [ID] | **Elizabeth N. H. Tran** | **Renato Morona**

Department of Molecular and Biomedical Sciences, Research Centre for Infectious Diseases, School of Biological Sciences, The University of Adelaide, Adelaide, South Australia, Australia

Correspondence
Nicholas Maczuga, Department of Molecular and Biomedical Sciences, Research Centre for Infectious Diseases, School of Biological Sciences, The University of Adelaide, Adelaide, SA, Australia.
Email: nicholas.maczuga@adelaide.edu.au

Abstract

Enterobacterales have developed a specialized outer membrane polysaccharide (enterobacterial common antigen [ECA]). ECA biosynthesis begins on the cytoplasmic side of the inner membrane (IM) where glycosyltransferases sequentially add sugar moieties to form a complete repeat unit which is then translocated across the IM by WzxE before being polymerized into short linear chains by WzyE/WzzE. Research into WecG, the enzyme responsible for generating ECA lipid-II, has not progressed beyond Barr et al. (1988) who described WecG as a membrane protein. Here we revise our understanding of WecG and re-characterize it as a peripherally associated membrane protein. Through the use of Western immunoblotting we show that WecG in *Shigella flexneri* is maintained to the IM via its three C-terminal helices and further identify key residues in helix II which are critical for this interaction which has allowed us to identify WecG as a GT-E glycosyltransferase. We investigate the possibility of protein complexes and ultimately show that ECA lipid-I maintains WecG to the membrane which is crucial for its function. This research is the first since Barr et al. (1988) to investigate the biochemistry of WecG and reveals possible novel drug targets to inhibit WecG and thus ECA function and cell viability.

KEYWORDS
ECA, glycosyltransferase, GT-E, WecG

1 | IMPORTANCE

ECA has been shown to play major roles in the homeostasis of cells as mutants along its biosynthetic pathway, particularly its glycosyltransferases have been shown to induce pleiotropic phenotypes as well as induce cell wall stress pathways (Castelli & Vescovi, 2011; Jorgenson et al., 2016). Due to this, research into the roles that the ECA glycosyltransferases play in these pleiotropic phenotypes has dominated ECA research with little research being performed in understanding the enzymes themselves. WecG research has not progressed since 1988 when it was first identified by Barr et al. who described WecG as a membrane protein. Here, we show that WecG is a peripheral membrane protein, maintained to the IM via interactions facilitated by its C-terminal tail. We describe a new model of how WecG is maintained to the IM and present WecG as the second protein in the novel glycosyltransferase-fold family, GT-E.

2 | INTRODUCTION

Enterobacterales, an order of bacteria belonging to Gram-negatives, have developed unique adaptations which allow them to persist and

---

Abbreviations: ECA, enterobacterial common antigen; Und-P, undecaprenyl phosphate.

cause disease in their specific environmental niches; one such adaptations is the production of the outer membrane (OM) polysaccharide enterobacterial common antigen (ECA). ECA is presented on the OM in two membrane-associated forms, ECA_{pg} and ECA_{lps}, where ECA polysaccharide chains are directly linked to either phosphatidylglycerol (pg) or the core-sugars of LPS, respectively (Gozdziewicz et al., 2015; Maciejewska et al., 2020). The membrane-associated forms of ECA has been shown to play crucial roles in maintaining OM homeostasis as well as providing resistance to bile salts (Castelli & Vescovi, 2011; Ramos-Morales et al., 2003). ECA additionally presents in a periplasmically restricted form, ECA_{cyc}, which contains no lipid anchor and but also acts to maintain the permeability barrier of the OM (Kajimura et al., 2005; Mitchell et al., 2018).

Universal in all Enterobacterales, ECA comprises of a trisaccharide repeating units (RUs) containing N-acetylglucosamine (GlcNAc), N-acetyl-D-mannosaminuronic acid (ManNAcA), and 4-acetamido-4,6-dideoxy-D-galactose (Fuc4NAc) with the biosynthesis of ECA commencing on the cytoplasmic side of the inner membrane (IM) (Eade et al., 2021). Briefly, UDP-GlcNAc is transferred onto the polyprenyl phosphate lipid carrier undecaprenyl phosphate (Und-P) by the glycosyltransferase WecA, generating ECA lipid-I (Al-Dabbagh et al., 2008). Sequential additions of ManNAcA and Fuc4NAc facilitated by WecG and WecF yield the complete ECA RU which is then translocated across the IM by WzxE (Eade et al., 2021). Lastly, ECA polysaccharide chains are assembled by WzyE and WzzE before the complete polysaccharide chain is ligated onto a final lipid anchor prior to export to the OM (Figure 1) (Islam & Lam, 2014).

Research into the glycosyltransferases (GT) of the ECA biosynthetic pathway has been orientated toward understanding the effects of mutations in their coding genes which cause pleiotropic mutant phenotypes through the accumulation of biosynthetic intermediates and sequestering Und-P from related pathways, with little work orientated in furthering our understanding of the enzymes themselves (Jorgenson et al., 2016; Ramos-Morales et al., 2003). WecG is one such glycosyltransferase which was extensively investigated for its role in cell wall mutants; however, research specifically into the enzyme has not progressed since Barr et al. (1988) at the time when the genes responsible for ECA biosynthesis were first being discovered and described (Barr et al., 1988; Danese et al., 1998; Jiang et al., 2020; Jorgenson et al., 2016).

WecG, a UDP-N-acetyl-D-mannosaminuronic acid transferase, facilitates the transfer of UDP-ManNAcA onto ECA lipid-I, generating ECA lipid-II and in the process of doing so, commits the biosynthetic intermediate to ECA biosynthesis as it is not utilized in other cellular pathways (Eade et al., 2021). Initial research into understanding WecG placed it as a membrane protein, as whole membranes from a $wecG^+$ strain were able to in vitro polymerise ECA using ECA lipid-I supplied from a $wecG^-$ mutant, observed as a restoration of ECA banding by anti-ECA Western immunoblotting (Barr et al., 1988). In this study we clarify WecG's localization in *Shigella flexneri* and show that WecG is not an integral membrane protein, but one which is strongly associated with the membrane through interactions facilitated with its in silico-predicted C-terminal helices.
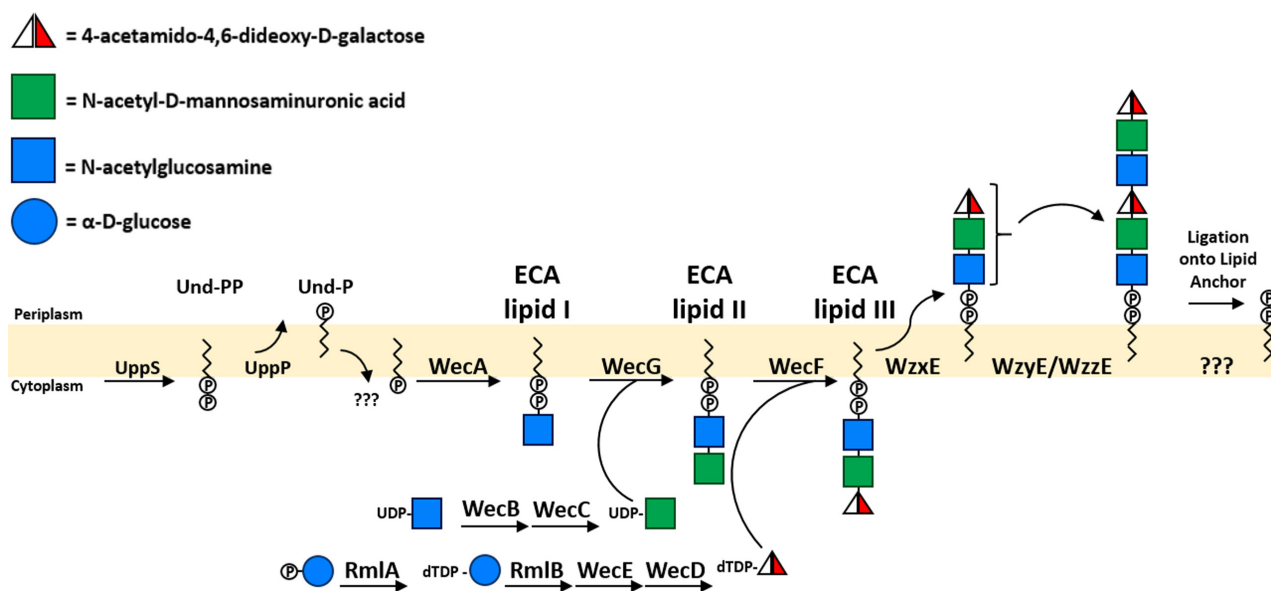

FIGURE 1 Enterobacterial common antigen biosynthesis in *Enterobacteriales*. ECA biosynthesis begins on the cytoplasmic side of the inner membrane (IM) where undecaprenyl phosphate (Und-P) is acted upon by WecA to yield Und-PP-GlcNAcA ECA lipid-I (Al-Dabbagh et al., 2008). The sequential addition of ManNAcA and Fuc4NAc by the glycosyltransferases WecG and WecF yield ECA lipid-II and ECA lipid-III, respectively, at which point the complete ECA repeat unit (RU) which is subsequently flipped onto the periplasmic leaflet of the IM by the flippase WzxE (Eade et al., 2021). The polymerase WzyE and co-polymerase WzzE then polymerize a linear ECA polysaccharide of controlled length followed by ligation of the ECA polysaccharide onto its final lipid carrier prior to export to the outer membrane (Woodward et al., 2010). The translocation of Und-P to the periplasmic side of the IM by UppP remains a speculative. Figure adapted from Maczuga et al. (2022a)

High peptide sequence homology with a novel GT-E fold protein TagA, a UDP-N-acetyl-D-mannosaminuronic acid transferase from Gram positives, suggested to us that WecG is a glycosyltransferase belonging to the novel GT fold family, GT-E (Kattke et al., 2019). Western immunoblotting of carboxy terminal (C-terminal) deletions of WecG showed that WecG's membrane association was depended on the presence of it's C-terminal helices which maintained WecG with the IM. Multiple sequence alignments identified conserved residues throughout the C-terminal helices which we showed are crucial for maintaining WecG to the membrane and ECA production which establish that WecG's functionality is dependent on its membrane association. Lastly we demonstrate that WecG's membrane association is dependent on the presence of ECA lipid-I, and present a hypothesis that WecG is primarily maintained to the membrane through interactions facilitated between crucial residues in its second C-terminal helix and ECA lipid-I.

This study provides a new understanding of the ECA biosynthetic pathway and the key enzyme which specifically initiates it, WecG. We clarify the long held model of ECA biosynthesis and show the extent of WecG's dependence on its membrane association and elucidate possible targets to block ECA production in Enterobacterales.

3 | MATERIALS AND METHODS

3.1 | Bacterial strains, growth media, and growth conditions

Bacterial strains and plasmids used in this study are listed in Table 1. Bacteria were routinely grown at 37°C in Lysogeny-Bertani (LB) broth with aeration or on LB agar (LBA). Antibiotics used were 100 μg ampicillin (Amp) ml^{-1} and 10 ng tunicamycin ml^{-1} with 3 μg polymyxin B nonapeptide ml^{-1} (PBMN; Sigma). Strains carrying pWKS30 requiring induction were grown in LB at 37°C with aeration for 16 h, sub-cultured (1/20) into fresh broth and induced with 1 mM isopropyl-β-D-thiogalactopyranoside (IPTG). Cultures were grown for a further for 4 h.

3.2 | DNA methods

The plasmids used in this study are presented in Table 1. Plasmid were purified from *E. coli* DH5α strains using a QIAprep Spin miniprep kit (Qiagen). Preparation of electrocompetent cells and electroporation methods were performed as described previously (Purins et al., 2008).

3.3 | Chromosomal mutagenesis

The *S. flexneri* Y PE860 Δ*wzyE*$_{10-440}$ strain was generated using λ Red mutagenesis as described in Datsenko and Wanner (2000). Briefly, DNA primers were designed to PCR amplify a chloramphenicol resistance cassette flanked with 50 bp of homologous sequence to *wzyE* such that once deleted, 30 nucleotides of the 5′ and 3′ coding regions of *wzyE* would remain. The purified PCR fragment was then electroporated into the parent PE860 strain carrying pKD46 to generate the mutant strains. The antibiotic resistance cassette was removed by the introduction of pCP20.

3.4 | Construct generation/DNA sequencing

Primers used for construct generation are listed in Table S1. Generation of pWKS30-His$_{10}$WecG, denoted as pHis$_{10}$WecG, was performed by inverse PCR using primers (NM126/127) to amplify a fragment of DNA containing *wecG* with the coding sequence for a amino-terminal His$_{10}$ epitope tag using pWKS30-WecG as a template. The linear fragment was 5′ phosphorylated via poly nucleotide kinase (Genebank) before being circularized using T4 DNA ligase (Genebank). Generation of C-terminal deletions of WecG was performed as above using inverse PCR and primers (WecG^{ΔIII}:NM130.1/NM132, WecG$^{ΔII+III}$:NM130.1/NM133, WecG^{ΔA}:NM130.1/NM131.1) to amplify DNA fragments containing *his$_{10}$wecG* deletions using pWKS30-His$_{10}$WecG as a template. The linear fragments were then treated as above. Generation of WecG helix II point mutations was performed via site-directed mutagenesis by inverse PCR, and primers (WecG^{L215E}:NM140/NM141, WecG^{L218E}:NM142/NM143, WecG^{L222E}:NM146/NM147) were used to PCR amplify DNA fragments using pWKS30-His$_{10}$WecG as a template. The linear fragments were treated as above. DNA sequencing was used to confirm all constructs and that post ligation, the *wecG* coding sequence remained in-frame.

3.5 | Whole cell protein sample preparation

Bacteria were grown and induced as described above before 5×10^8 cells were collected by centrifugation (2000*g*) and resuspended in 100 μl of 2× sample buffer (Lugtenberg et al., 1975). Samples were heated at 56°C for 10 min prior to loading.

3.6 | ECA sample preparation

Bacteria were grown and induced as described above before 1×10^9 cells were collected by centrifugation (2000*g*), resuspended in 2× lysis buffer (Murray et al., 2003), and heated at 100°C for 10 min before incubation with 2.5 mg/ml proteinase K (Sigma-Aldrich) for 2 h at 56°C. Samples were heated at 100°C for 1 min prior to loading.

3.7 | Membrane fractionation

Overnight cultures were subcultured into 200 ml LB and induced as above. Cultures were then pelleted via centrifugation (Beckman

Strain or plasmid	Description	Source
Strains		
RMA2162	*S. flexneri* PE860 Y serotype; strain lacks virulence plasmid and pHS-2 plasmid	Laboratory stock
NMRM120	*S. flexneri* PE860 $\Delta wzyE_{10\text{-}440}$	This study
NMRM344	*S. flexneri* PE860 $\Delta wecA$	Maczuga et al. (2022b)
NMRM348	*S. flexneri* PE860 $\Delta wecC$	Maczuga et al. (2022b)
RMA4622	*E. coli* K-12 BW25113	Laboratory stock
JW3770-1	*E. coli* K-12 BW25113 $\Delta wecG::Km$	Baba et al. (2006)
Plasmids		
pKD3	Source of Chloramphenicol resistance cassette for λ Red mutagenesis, Cml^r	Datsenko and Wanner (2000)
pKD46	Source of λ phage recombinase for homology recombination, 30°C growth for maintenance, 42°C for expression and cure, Amp^r	Datsenko and Wanner (2000)
pCP20	Source of yeast FRT specific recombinase for λ red mutagenesis, 30°C growth for maintenance, 42°C for expression and cure, Amp^r	Datsenko and Wanner (2000)
pWKS30	IPTG inducible, expression vector, Amp^r	Wang and Kushner (1991)
pWKS30-WecG	pWKS30 encoding WecG, Amp^r	This study
pHis$_{10}$WecG	pWKS30 encoding His$_{10}$WecG, Amp^r	This study
pHis$_{10}$WecG$^{\Delta A}$	pWKS30 encoding His$_{10}$WecG$^{\Delta A}$, Amp^r	This study
pHis$_{10}$WecG$^{\Delta II+III}$	pWKS30 encoding His$_{10}$WecG$^{\Delta II+III}$, Amp^r	This study
pHis$_{10}$WecG$^{\Delta III}$	pWKS30 encoding His$_{10}$WecG$^{\Delta III}$, Amp^r	This study
pHis$_{10}$WecG^{L215E}	pWKS30 encoding His$_{10}$WecG^{L215E}, Amp^r	This study
pHis$_{10}$WecG^{L218E}	pWKS30 encoding His$_{10}$WecG^{L218E}, Amp^r	This study
pHis$_{10}$WecG^{L222E}	pWKS30 encoding His$_{10}$WecG^{L222E}, Amp^r	This study

Coulter Avanti J-26 XPI centrifuge; 9600*g*, 10 min, 4°C) before resuspension in 10 ml of sonication buffer (100 mM NaCO$_3$ pH 7.0) and disrupted by sonication (Branson B15). Cellular debris was then collected and removed via centrifugation (Thermo Scientific Labofuge 400 R centrifuge; 3500*g*, 10 min, 4°C) prior to whole membrane (WM) collection by ultracentrifugation (Beckman Coulter Optima L-100 XP ultracentrifuge; 250,000*g*, 45 min, 4°C). WM were then resuspended in 5 ml of MQ at 4°C.

3.8 | Dissociation assays

Briefly, 500 μl of WMs were aliquoted into 1.5 ml reaction tubes to which 500 μl of various solutions were added (3 M NaI 200 mM NaCO$_3$ pH 7.0; 4 M NaCl 200 mM NaCO$_3$ pH 7.0; 200 mM NaCO$_3$ pH 12.0; 200 mM NaCO$_3$ pH 7.0 or PBS). The reaction tubes were then incubated at room temperature for 1 h with agitation before the insoluble faction membrane was collected via ultracentrifugation as above.

3.9 | In vivo DSP crosslinking

Overnight bacterial cultures were sub-cultured (1/20) into 200 ml fresh LB broth, induced as above and grown for a further 4 h. Cells were then collected via centrifugation as above, washed, and resuspended in 5 ml DSP-Crosslinking buffer (150 mM NaCl, 20 mM Na$_2$PO$_4$/NaH$_2$PO$_4$, pH 7.2) prior to incubation with 1 mM DSP (Thermo fisher Scientific) for 30 min at 37°C (+DSP samples). A duplicate sample was also incubated for 30 min at 37°C without treatment (−DSP samples). Excess DSP was then quenched using 20 mM Tris–HCl, pH 7.5 for 10 min at room temperature prior to collection and resuspension in sonication buffer as above.

3.10 | Western immunoblotting

Protein/ECA samples were loaded onto a 12% or 15% SDS–PAGE gel, respectively, and electrophoresed at 200 V for 1 h. SDS–PAGE gels were then transferred onto a nitrocellulose membrane (Bio-Rad)

at 400 mA for 1 h prior to membranes being blocked with 5% (wt/vol) skim milk in Tris–Tween Buffer saline (TTBS). Membranes were then incubated overnight with either monoclonal mouse anti-His antibodies (GenScript) (1:50,000), polyclonal rabbit anti-WzzE (1:500), or polyclonal rabbit anti-ECA antibodies (1:500), diluted in 2.5% (wt/vol) skim milk in TTBS. Detection was performed with rabbit anti-mouse or goat anti-rabbit horseradish peroxidase-conjugated antibodies (KLP) and chemiluminesence reagent (Sigma). A volume of 5 μl of SeeBlue Plus2 pre-stained protein ladder (Invitrogen) was used as a molecular mass standard.

3.11 | Bioinformatics analysis

The peptide sequence of WecG was obtained from NCBI (GenBank: CP042980.1). The WecG peptide sequence was then submitted to: TMHMM to in silico predict transmembrane helices, Jpred to in silico predict secondary structures and I-TASSER, Alphafold and RaptorX servers to in silico predict the tertiary structure of WecG (Drozdetskiy et al., 2015; Jumper et al., 2021; Källberg et al., 2012; Krogh et al., 2001; Yang et al., 2015). Multiple sequence alignments were performed in Jalview (Amar et al., 2018).

4 | RESULTS

4.1 | Bioinformatics analysis of WecG

Initial research on the localization of WecG performed by Barr et al. (1988) stated that WecG was a membrane protein. Since that initial study, there has been little research on the structure and subcellular localization of WecG, hence we first applied a bioinformatics approach to investigate the biophysical characteristics of WecG and its structure. The TMHMM (Krogh et al., 2001), Jpred (Drozdetskiy et al., 2015), I-TASSER (Yang et al., 2015), Alphafold (Jumper et al., 2021), and RaptorX (Källberg et al., 2012) servers were used to investigate the probability of transmembrane helices, the general secondary structure of WecG as well as to generate in silico predicted structures of WecG. Firstly, TMHMM predicted that WecG contained no transmembrane helices and Jpred predicted that WecG consists of 11 alpha helices and 8 beta sheets but none long enough to traverse a membrane as well as a possible single Rossmann fold with its characteristic alternating α-helices and β-sheets (Figure S1) (Bottoms et al., 2002; Saidijam et al., 2018). I-TASSER, Alphafold, and RaptorX gave a predicted protein structure of a globular protein consisting of a single Rossmann fold but no parallel alpha helices, which is the characteristic of transmembrane segments (Figure 2a–c). Additionally, once structurally compared it was observed that I-TASSER and RaptorX predicted a disordered C terminal domain (CTD), whereas Alphafold predicted three C terminal helices (Figure 2d) which was consistent with the prediction provided by Jpred (Figure S1). Interestingly, I-TASSER and RaptorX both independently produced

a model using the template protein TagA, with a TM score of 0.62+/−0.14 and p-value of 8.03e-30, respectively, which indicated a high structural similarity to TagA. TagA, a UDP-N-acetyl-D-mannosaminuronic acid transferase present in Gram positive *Thermoanaerobacter italicus* and *Staphylococcus aureus*, is a member of the Pfam glycosyltransferase WecG/TagA/CpsF family (PF03808) and is involved in the biosynthesis of wall teichoic acids (WTAs) (Swoboda et al., 2010).

4.2 | WecG associates with the membrane

To investigate the localization of WecG, a poly-His epitope tagged WecG expression construct was made. Initial attempts to generate a poly-his tagged WecG proved difficult as a WecG$_{His12}$ C-terminal His$_{12}$ tag construct could complement the *E. coli* BW25113 *ΔwecG::km* strain but could not be detected (Figure S2). An alternative N-terminal domain His$_{10}$ tagged WecG construct, pHis$_{10}$WecG, was made and transformed into *E. coli* BW25113 *ΔwecG::km* where it showed complementation of ECA and the protein was detected in whole cells (WC) via anti-His Western immunoblotting (Figure S2).

To investigate WecG's localization, membrane fractionation was performed on induced *S. flexneri* PE860 carrying pHis$_{10}$WecG (Figure 3a). A band of ~30 kDa which correlated to the expected mass of His$_{10}$WecG was detected in both the WC (Figure 3a, lane 1) and the whole membrane (WM) samples (Figure 3a, lane 3), which indicated that His$_{10}$WecG associated with the membrane.

Peripherally associated membrane proteins can be dissociated from the membrane by treatment with chaotropic agents, high salt, and high pH solutions (Smith, 2017). Therefore, to further investigate WecG's localization, WM samples were treated with a range of chemicals and conditions including 1.5 M NaI, 1 M NaCl and pH 12 in an attempt to dissociate WecG from the WM. As seen in Figure 3b, His$_{10}$WecG consistently associated with the WM as the treatments used did not dissociate His$_{10}$WecG from the WM samples.

4.3 | Peripheral association of WecG with the membrane is facilitated via CTD helices

A plausible explanation as to how WecG is associated with the membrane, while displaying no typical membrane protein predicted secondary folding and structure, could be that WecG is maintained at the membrane through interactions facilitated between its three predicted C-terminal alpha helices in a similar way to TagA (Kattke et al., 2019). To investigate this, three C-terminal domain (CTD) deletions were generated in pHis$_{10}$WecG; pHis$_{10}$WecG^{ΔA} which consisted of WecG with no CTD alpha helices, pHis$_{10}$WecG$^{ΔII+III}$ which consisted of WecG and its first CTD alpha helix, and pHis$_{10}$WecG^{ΔIII} which consisted of WecG and its first and second CTD alpha helix (Figure 4a,b). The constructs
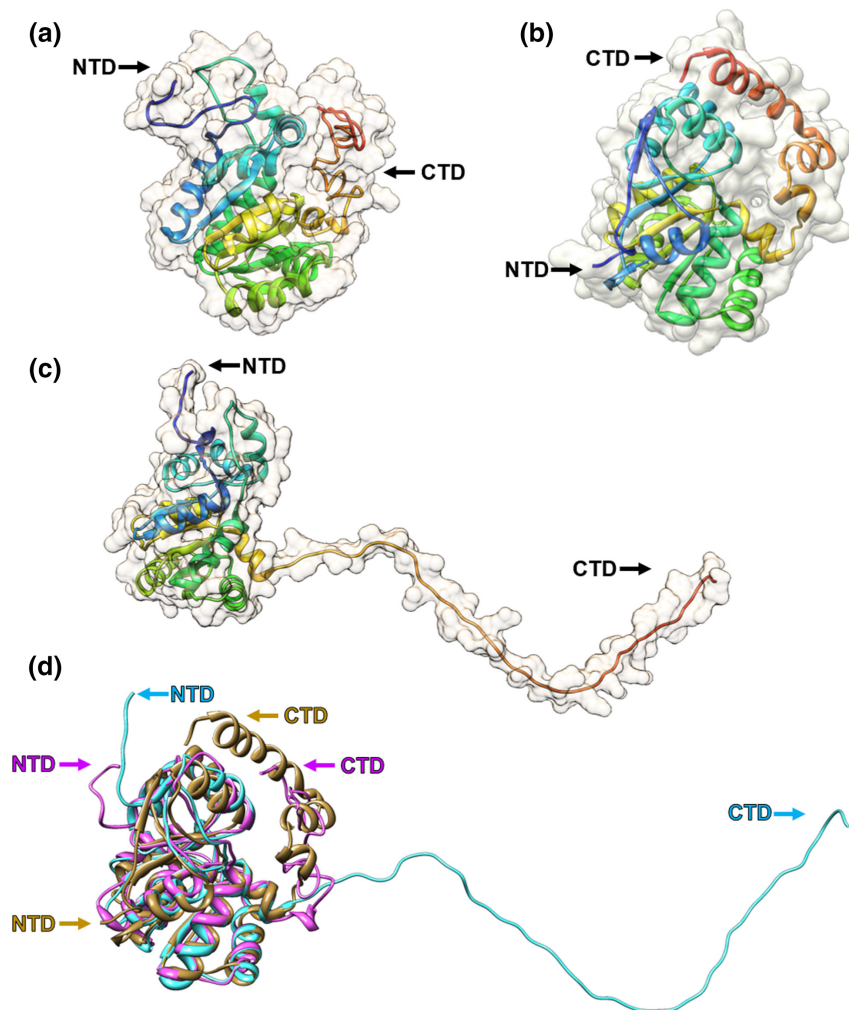
FIGURE 2 In silico predicted tertiary structures of WecG. (a) I-TASSER predicted structure of WecG suggests that WecG is a globular protein with an unorganized CTD. (b) Alphafold predicted structure of WecG shows that WecG is a globular protein with three CTD helices. (c) RaptorX predicted structure of WecG indicates that the structure of WecG consists of a globular NTD and a protruding CTD. (d) Structural overlay comparison of WecG predicted models from I-TASSER in pink, Alphafold in gold, and RaptorX in blue. NTD = amino terminal domain, CTD = carboxyl terminal domain

were then tested to determine what effect the CTD deletions had on WecG's membrane association by membrane fractionation. As seen in Figure 4c, deletion of WecG CTD helix I and II caused WecG to dissociate from the membrane as His_{10}WecG bands were only present in the supernatant (SN) samples (Figure 4c, lanes 4 and 6); however, deletion of WecG's third CTD helix did not affect WecG's association with the membrane fraction as a His_{10}WecG band was present in the WM sample (Figure 4c, lane 7). This supported the hypothesis that WecG's CTD play an important role in maintaining WecG membrane association and revealed that helix II plays an essential role as its deletion appeared to cause WecG to dissociate from the membrane.

We further investigated what impact the CTD deletions had on WecG's function in ECA biosynthesis by complementing the *E. coli* BW25113 *ΔwecG::km* mutant with $pHis_{10}WecG^{ΔA}$, $pHis_{10}WecG^{ΔII+III}$, and $pHis_{10}WecG^{ΔIII}$ and determining ECA production via Western immunoblotting. The three WecG CTD deletions mutants were unable to complement the BW25113 *ΔwecG::km* mutant (Figure 4d, lanes 5–7) leading us to hypothesize that key catalytic domains are at least partially formed by the three CTD helices of WecG which would be in accordance with observations in TagA (Kattke et al., 2019). The deletion not only

disrupts this catalytic domain but also causes WecG to dissociate from the membrane.

4.4 | Key hydrophobic residues in WecG CTD helix II facilitate membrane association

During the bioinformatic analysis of WecG, it was observed that a series of conserved hydrophobic residues lie along the same face of WecG's CTD helix II, taking 3.6 amino acid residues per turn (Figure 5a). This led us to hypothesize that the association of WecG to the membrane could be facilitated by these residues. Amino acid substitutions were generated in $pHis_{10}$WecG to determine the importance of the residues L215, L218, and L222, as described in the methods.

The resulting constructs ($pHis_{10}WecG^{L215E}$, $pHis_{10}WecG^{L218E}$, and $pHis_{10}WecG^{L222E}$) were transformed into *S. flexneri* PE860 and *E. coli* BW25113 *ΔwecG::km* to assess the effect on WecG's subcellular localization as well as any effect on ECA biosynthesis (Figure 1). As seen in Figure 5b,c, substitutions of L215E did affect the subcellular localization of $His_{10}WecG^{L215E}$ as a protein band was present in both the WM and SN samples (Figure 5b,c lanes 8 & 9). However
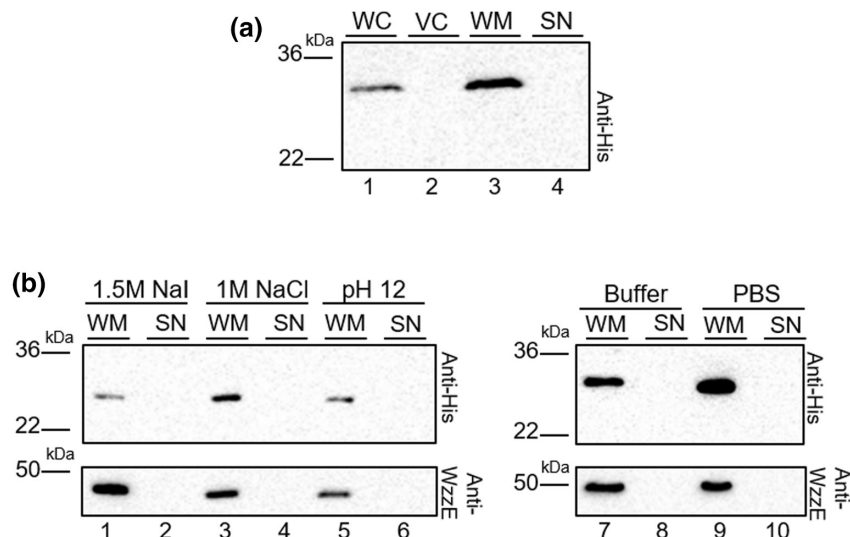
FIGURE 3 Subcellular localization of His$_{10}$WecG in *Shigella flexneri* PE860. (a) Anti-his Western immunoblot of His$_{10}$WecG subcellular localization expressed from PE860. Mid-exponential phase cells were disrupted by sonication and WM were collected by ultracentrifugation. Samples were electrophoresed on a SDS-12% (w/v) PAGE gel followed by immunoblotting with anti-his antibodies. (b) Anti-his and anti-WzzE Western immunoblot of chemical treated WMs from PE860 cells expressing pHis$_{10}$WecG. WM were collected as above and were incubated 1:1 with 3 M NaI, 2 M NaCl or pH 12 buffer before membranes were collected by ultracentrifugation. Samples were electrophoresed as above prior to immunoblotting with anti-his or anti-WzzE antibodies. WC = whole cell, VC = vector control, WM = whole membrane, SN = supernatant. SeeBlue Plus2 pre-stained protein ladder (Invitrogen) was used as a molecular mass standard

the substitution of L218E caused the complete dissociation of His$_{10}$WecG^{L218E} from the membrane as no protein bands were present in the membrane fraction (MF) sample but were present in the S/N sample(compare Figure 5b,c lanes 11&12). The substitution of L222E resulted in His$_{10}$WecG^{L222E} partially dissociating from the membrane as protein bands were detected in both the WM and S/N samples (compare Figure 5b,c lanes 14 & 15).

To assess what effect these mutational alterations had on ECA biosynthesis, an anti-ECA Western immunoblot was performed (Figure 5d). Mutant His$_{10}$WecG^{L215E} had minimal effect on ECA banding (Figure 5d, lane 5) as the ECA banding profile showed slightly less intensity when compared with the His$_{10}$WecG complemented strain (Figure 5d, lane 4). The mutants His$_{10}$WecG^{L218E} and His$_{10}$WecG^{L222E} however had a drastic effect on ECA biosynthesis as the His$_{10}$WecG^{L218E} mutant was unable to complement the *wecG* mutant, seen as the lack of ECA banding (Figure 5d, lane 6) and the His$_{10}$WecG^{L222E} mutant was only partially able to complement the *wecG* mutant (Figure 5d, lane 7), detected as low intensity reduced the length of ECA banding. This profile data supported the hypothesis that residues L218 and L222 were crucial for WecG membrane association which in turn appeared to be crucial for ECA biosynthesis.

4.5 | WzyE polymerase mutation decreases WecG's membrane association

WecG is translationally coupled to WzyE as *wecG*'s ribosomal binding site (RBS) lies within the 3′ end of *wzyE*'s coding region (Figure 6a). It has been proposed in the past that the proteins involved in

the Wzy-dependent pathway form a protein complex (Islam & Lam, 2014; Marolda et al., 2006), hence the impact of WzyE on WecG's membrane association was investigated. The pHis$_{10}$WecG plasmid was transformed into PE860 and PE860 Δ*wzyE*$_{10-440}$ following which cell fractionations were performed (Figure 6b). His$_{10}$WecG was detected in the WM samples of PE860 Δ*wzyE*$_{10-440}$ (Figure 6b, lane 3), indicating that in the absence of WzyE, WecG still associates with the membrane. To further investigate the impact of WzyE, WMs from PE860 *wzyE*$_{10-440}$ mutant expressing pHis$_{10}$WecG were chemically treated post fractionation as above to attempt to dissociate His$_{10}$WecG from the membrane. Unexpectedly, unlike in PE860 (Figure 3b, lane 2), the presence of 1.5 M NaI induced the partial dissociation of His$_{10}$WecG from the WM of the PE860 *wzyE*$_{10-440}$ mutant strain (Figure 6c, lane 3).

To investigate the possibility that WzyE physically interacts with WecG to maintain WecG's peripheral membrane association, DSP crosslinking was performed on the whole cells. As seen in Figure 6d, crosslinking with DSP showed no band shifts for His$_{10}$WecG in both the PE860 and *wzyE*$_{10-440}$ mutant strains, indicating that WecG does not detectably interact with WzyE or any other protein.

4.6 | Lipid interactions are crucial for WecG's association with the membrane

As no physical protein–protein interaction was detected via DSP crosslinking as described above, it was hence hypothesized that WecG may be primarily maintained to the membrane through lipid-mediated interactions between itself and ECA lipid-I and/or lipid-II (Figure 1). To investigate if ECA biosynthetic intermediates instead
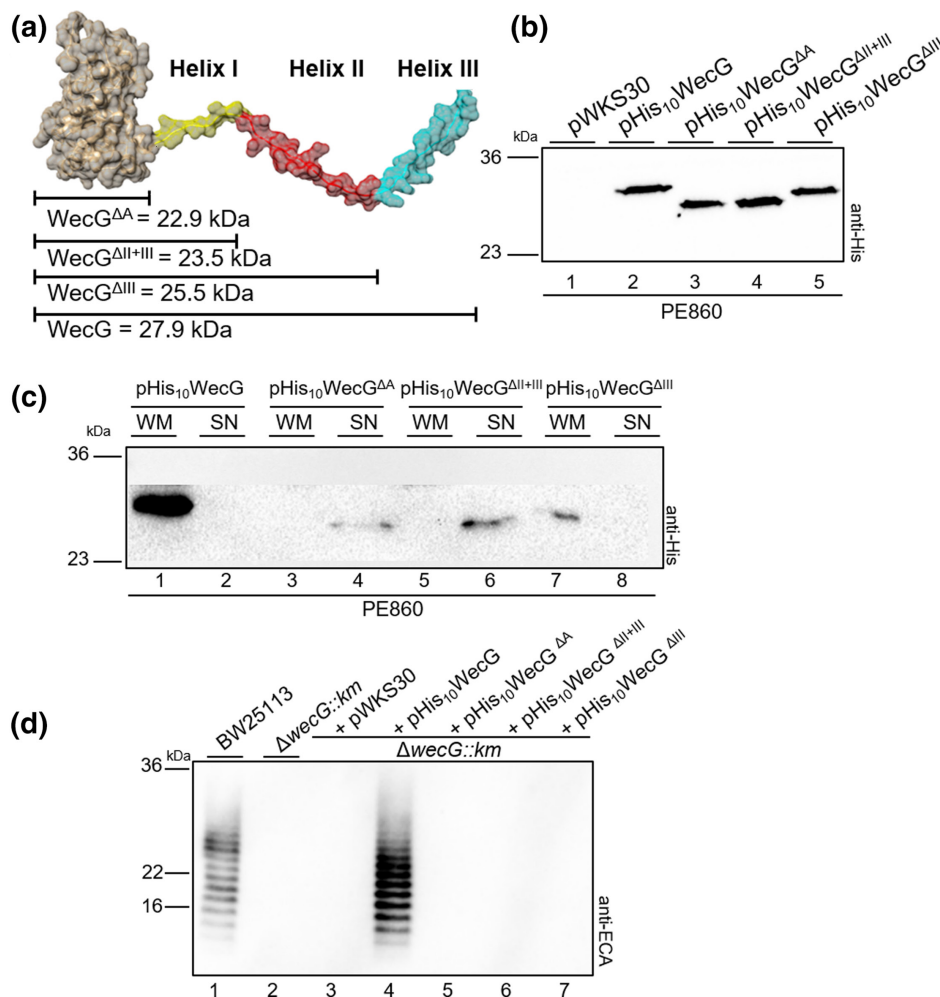
FIGURE 4 WecG CTD helices are crucial in maintaining WecG's peripheral association with the membrane and ECA production. (a) Model of WecG based on TagA derived by RaptorX showing the location and structure of WecG CTD deletion mutations. (b) Anti-His Western immunoblot of whole cell samples from PE860 strains harboring pHis$_{10}$WecG, pHis$_{10}$WecG$^{\Delta A}$, pHis$_{10}$WecG$^{\Delta II+III}$ and pHis$_{10}$WecG$^{\Delta III}$. Mid-exponential phase cells were collected (5×10^8 cells) and lysed in lysis buffer. Samples were electrophoresed on a SDS-12% (w/v) PAGE gel, transferred onto a nitrocellulose membrane, and probed with anti-his antibodies. (c) Anti-his Western immunoblot of the subcellular location of the WecG CTD mutants. PE860 cells harboring pWKS30, pHis$_{10}$WecG, pHis$_{10}$WecG$^{\Delta A}$, pHis$_{10}$WecG$^{\Delta II+III}$, and pHis$_{10}$WecG$^{\Delta III}$ were disrupted and membranes were collected by ultracentrifugation. WM samples were electrophoresed on a SDS-12% (w/v) PAGE gel followed by immunoblotting with anti-his antibodies. WM = whole membrane, SN=supernatant. (d) Anti-ECA Western immunoblot showing ECA production from *E. coli K-12* BW25113 *ΔwecG::Km* strains harboring pWKS30, pHis$_{10}$WecG, pHis$_{10}$WecG$^{\Delta A}$, pHis$_{10}$WecG$^{\Delta II+III}$ and pHis$_{10}$WecG$^{\Delta III}$. Mid-exponential phase cells were collected (1×10^9 cells) by centrifugation and lysed in lysis buffer in the presence of proteinase K. samples were electrophoresed on a SDS-15% (w/v) PAGE gel followed by immunoblotting with anti-ECA antibodies. SeeBlue Plus2 pre-stained molecular weight ladder (Invitrogen) was used as a molecular weight marker for (b) to (d)

FIGURE 5 Key residues within WecG's CTD helix II play crucial roles in WecG's peripheral association with the membrane and ECA production. (a) Local multiple sequence alignment from Jalview (Waterhouse et al., 2009) of WecG with other UDP-N-acetyl-D-mannosaminuronic acid transferases. The three CTD helices show a high level of sequence identity with multiple residues remaining entirely conserved. Coloration based off of residue hydrophobicity where red indicates hydrophobic and blue indicates hydrophilic (b) anti-his Western immunoblot of the subcellular localization of His$_{10}$WecG substitution mutants from PE860 cells harboring pWKS30, pHis$_{10}$WecG^{L215E}, pHis$_{10}$WecG^{L218E}, and pHis$_{10}$WecG^{L222E}. Mid-exponential phase cells were disrupted and membranes were collected by ultracentrifugation. Samples were electrophoresed on a SDS-12% (w/v) PAGE gel followed by immunoblotting with anti-his antibody. (c) Anti-his Western immunoblot of the subcellular localization of His$_{10}$WecG substitution mutants from BW25113 *ΔwecG::Km* cells harboring pWKS30, pHis$_{10}$WecG^{L215E}, pHis$_{10}$WecG^{L218E}, and pHis$_{10}$WecG^{L222E}. Mid-exponential phase cells were disrupted and membranes were collected by ultracentrifugation. Samples were electrophoresed on a SDS-12% (w/v) PAGE gel followed by immunoblotting with anti-his antibody. (d) Anti-ECA Western immunoblot of His$_{10}$WecG substitution mutant's effect on ECA biosynthesis in BW25113 *ΔwecG::Km* strains harboring pWKS30, pHis$_{10}$WecG^{L215E}, pHis$_{10}$WecG^{L218E}, and pHis$_{10}$WecG^{L222E}. Mid-exponential phase cells were collected (1×10^9 cells) by centrifugation and lysed in lysis buffer in the presence of proteinase K. Samples were electrophoresed on a SDS-15% (w/v) PAGE gel followed by immunoblotting with anti-ECA antibodies. SeeBlue Plus2 pre-stained molecular weight ladder (Invitrogen) was used as a molecular weight marker for (b) to (d). WC = whole cell, WM = whole membrane, SN = supernatant

affected WecG's membrane association, treatment with tunicamycin was used to block the production of ECA lipid-I by inhibiting WecA (Heifetz et al., 1979). Wildtype PE860 cells expressing pHis$_{10}$WecG were treated with 10 ng/ml tunicamycin, fractionated and WMs chemically treated as above. Unlike the attempts at dissociation of His$_{10}$WecG by chemical treatments (Figure 3b), treatment
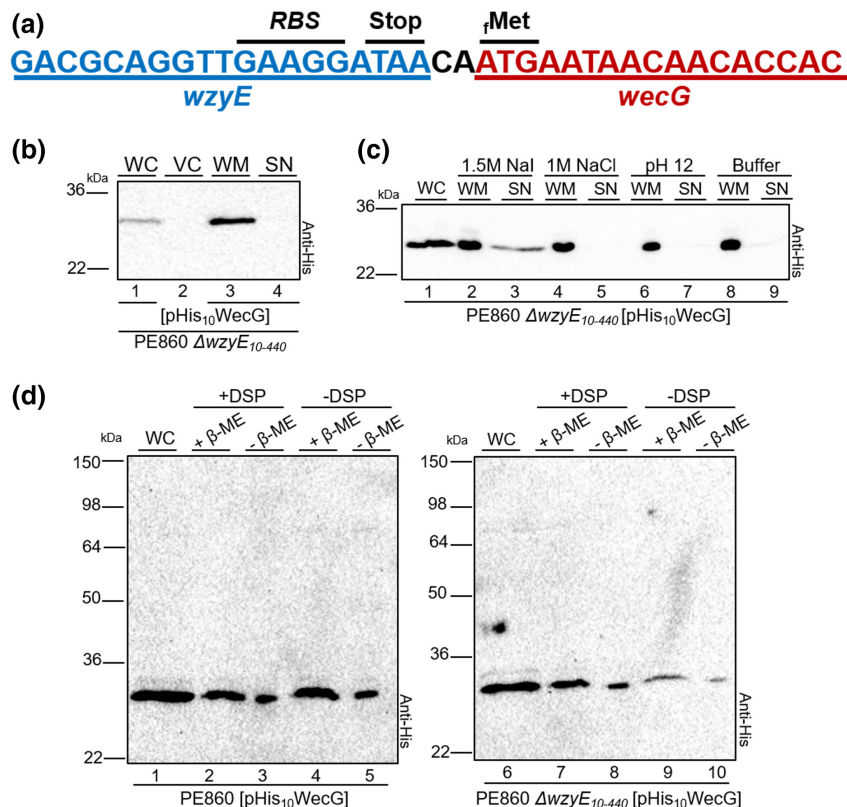
(a)

(b)

(c)

(d)
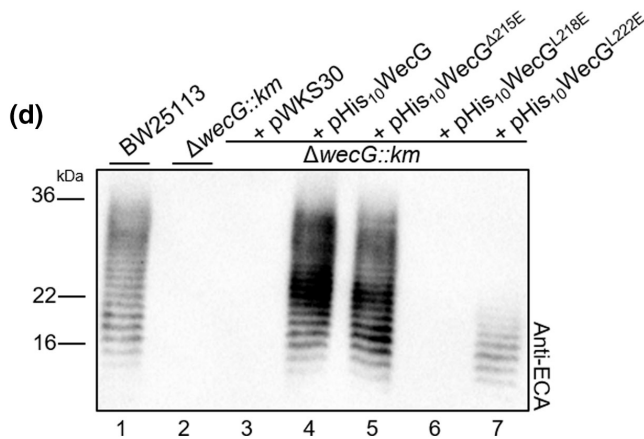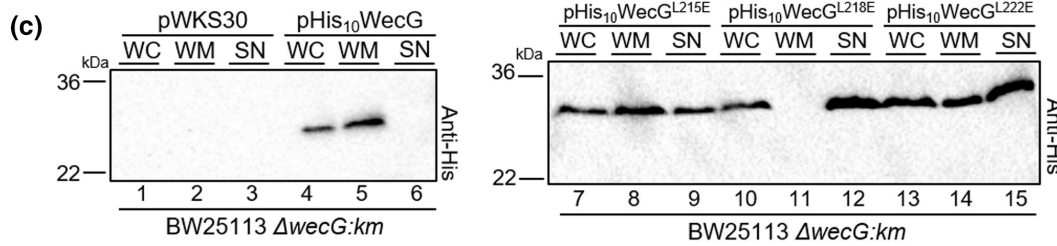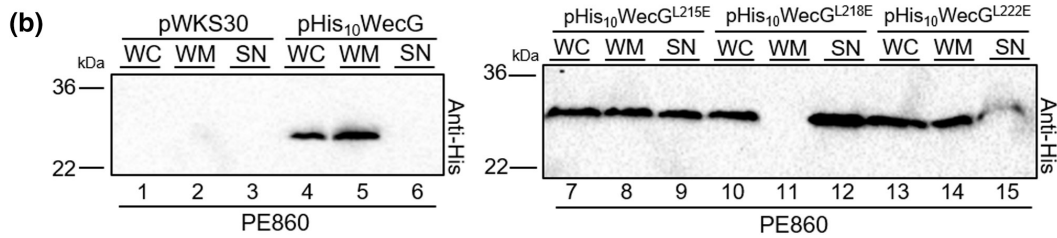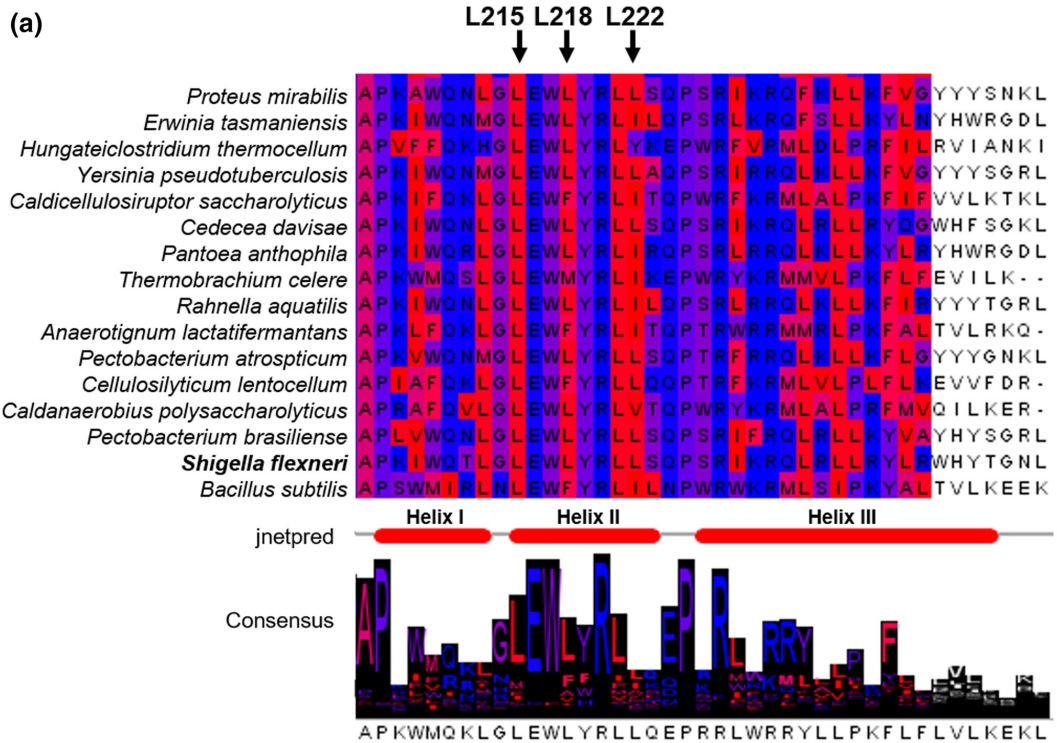
FIGURE 6 Effect of WzyE on WecG's peripheral membrane association. (a) Genetic arrangement of *wzyE* and *wecG* in *S. flexneri*. (b) Anti-his Western immunoblot of the subcellular localization of His_{10}WecG in PE860 $\Delta wzyE_{10-440}$. Mid-exponential phase cells were disrupted by sonication and WM were collected by ultracentrifugation. Samples were electrophoresed on a SDS-12% (w/v) PAGE gel followed by immunoblotting with anti-his antibodies. WC = whole cell, VC = vector control, WM = whole membrane, SN = supernatant. (c) Western immunoblot of chemical treated WMs from PE860 $\Delta wzyE_{10-440}$ cells expressing $pHis_{10}$WecG. WM were collected as above and were incubated 1:1 with 3 M NaI, 2 M NaCl or pH 12 buffer before membranes were collected by ultracentrifugation. Samples were electrophoresed on a SDS-12% (w/v) PAGE gel followed by immunoblotting with anti-his antibodies. (d) Anti-his Western immunoblot of DSP treated PE860 and PE860 $\Delta wzyE_{10-440}$ cells expressing $pHis_{10}$WecG. Mid-exponential phase cells were treated with 0.1 M DSP and quenched with 1 M tris HCl prior to the addition of sample buffer with and without β-ME. Samples were electrophoresed on a SDS-12% (w/v) PAGE gel followed by immunoblotting with anti-his antibodies. SeeBlue Plus2 pre-stained molecular weight ladder (Invitrogen) was used as a molecular weight marker for (b) to (d)

with tunicamycin caused the dissociation of His_{10}WecG from the MF in all treatment samples (Figure 7a, lanes 1–9). As tunicamycin inhibits both WecA and MraY albeit with drastically different MICs (Takatsuki et al., 1971), His_{10}WecG was expressed in a PE860 *wecA* mutant strain to further clarify if the effects of tunicamycin treatment was due to off target effects namely on MraY and peptidoglycan biosynthesis. Expression in the PE860 *wecA* mutant strain showed that while the majority of the protein was in the WM fraction, some was detected in the SN (Figure 7b, lanes 3 and 4), mirroring to the result observed with tunicamycin treatment. This strongly supported the hypothesis that WecG is indeed peripherally maintained to the membrane through strong, lipid mediated interactions. To determine whether this peripheral interaction is facilitated by ECA lipid-I or ECA lipid-II, $pHis_{10}$WecG was transformed into PE860 $\Delta wecC$ as *wecC* mutants are known to interrupt the ECA biosynthetic pathway and prevent the biosynthesis of ECA lipid-II (Figure 1). As seen in Figure 7c, none of the treatments were able to dissociate His_{10}WecG from the whole membrane of the *wecC* mutant, leading

us to hypothesize that WecG is maintained to the membrane through lipid interactions involving ECA lipid-I.

5 | DISCUSSION

Glycosyltransferases play crucial roles in the biogenesis of the cellular envelope. WecG, which is involved in ECA biosynthesis, facilitates the addition of UDP-N-acetyl-D-mannosaminuronic acid to ECA lipid-I, generating ECA lipid-II (Meier-Dieter et al., 1990). Here, we clarified historic observations of WecG (Barr et al., 1988), demonstrating that WecG is in fact a peripheral membrane protein and present WecG as the second protein belonging to the novel glycosyltransferase fold family, GT-E (Mestrom et al., 2019).

Our study shows for the first time the presence and importance of WecG's C-terminal helices in maintaining WecG to the membrane. The importance of the C-terminal helices in GT-E fold proteins was previously demonstrated by Kattke et al. (2019) who similarly
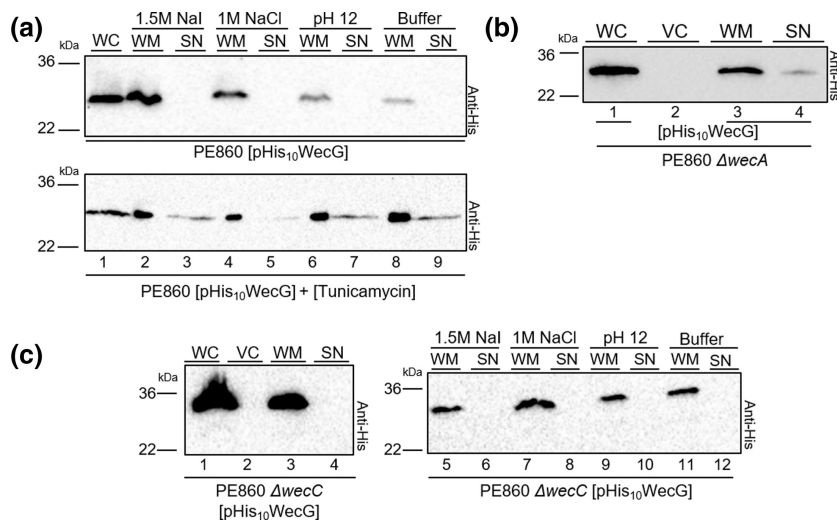
FIGURE 7 Investigating the role of lipids in WecG's peripheral membrane association. (a) Anti-his Western immunoblot of PE860 cells expressing pHis$_{10}$WecG treated with and without tunicamycin. Mid-exponential phase cells were grown in the presence of 10 ng/ml tunicamycin and 3 μg/ml PMBN. Cells were then disrupted and membranes collected by ultracentrifugation, following which WMs were incubated 1:1 with 3 M NaI, 2 M NaCl or pH 12 buffer before membranes were collected by ultracentrifugation. Samples were electrophoresed on a SDS-12% (w/v) PAGE gel followed by immunoblotting with anti-his antibodies. (b) Anti-his Western immunoblot of PE860 Δ*wecA* cells expressing pHis$_{10}$WecG. Mid-exponential phase cells were disrupted by sonication and WM were collected by ultracentrifugation. Samples were electrophoresed on a SDS-12% (w/v) PAGE gel followed by immunoblotting with anti-his antibodies. (c) Anti-his Western immunoblot of PE860 Δ*wecC* cells expressing pHis$_{10}$WecG. Mid-exponential phase cells were disrupted and membranes collected by ultracentrifugation. Chemical treatment of WM samples were performed as above. Samples were electrophoresed on a SDS-12% (w/v) PAGE gel prior to immunoblotting with anti-his antibodies. WC = whole cell, VC = vector control, WM = whole membrane, SN = supernatant. SeeBlue Plus2 pre-stained molecular weight ladder (Invitrogen) was used as a molecular weight marker for (a-c)

demonstrated their role in maintaining TagA's membrane association as well as in forming TagA's catalytic domain (Kattke et al., 2019). Their importance was shown through the use of chemical treatments, CTD deletions, and nucleotide substitutions to dissociate TagA from the membrane (Kattke et al., 2019).

Employing a similar approach in this study, we demonstrated that unlike TagA which was dissociated from membranes using 1.5 M NaI or 0.1 N KOH (Kattke et al., 2019), WecG cannot be dissociated from the membrane through the use of chemical treatments (Figure 3b). CTD deletions revealed that WecG's helix II is crucial for maintaining WecG's membrane association however, all three helices are required for ECA production (Figure 4c,d). Further, using a local multiple sequence alignment from a diverse range of phylogenetically distinct species, we focused on WecG's helix II and identified conserved leucine residues L215, L218, and L222. We then demonstrated their crucial roles in WecG's membrane association of as well as ECA production (Figure 5b–d) where, His$_{10}$WecG^{L218E} completely dissociated from the membrane and the substitutions of His$_{10}$WecG^{L215E} and His$_{10}$WecG^{L222E} induced a partial dissociation from the membrane (Figure 5b,c).

Complementation assays using the *E. coli* K-12 BW25113 Δ*wecG::km* strain revealed the inability of the L218E mutant and the partial ability of the L222E mutant to complement the ECA production in the *wecG* mutant (Figure 5d). These results suggested that WecG's CTD helices are involved in two distinct roles; in WecG's membrane association and also in WecG's catalytic activity where L218 and L222 potentially play critical roles. The formation of the

catalytic domain facilitated by the CTD helices is a common feature in GT-E-fold glycosyltransferases as TagA's catalytic domain also is facilitated by its CTD helices (Kattke et al., 2019).

We also investigated other possible factors which could contribute to maintaining WecG's membrane association. In the absence of WzyE, WecG could be dissociated from the WM by treatment with 1.5 M NaI (Figure 6c). This dissociation could have been induced due to the absence of a physical interaction between WzyE and WecG. Alternatively, it is known that mutants of the *wec* operon induce morphological abnormalities in cells due to the build-up of dead-end biosynthetic precursors (Jorgenson et al., 2016). As such, it is plausible that a build-up of biosynthetic precursors due to the reduced ECA lipid-III usage in *wzyE* mutant could have interrupted lipid mediated interactions between WecG and ECA biosynthetic precursors, namely ECA lipid-I or ECA lipid-II (Figure 1) (Maczuga et al., 2022b).

To investigate these possibilities, DSP crosslinking and chemical treatment of cells with 10 ng/ml tunicamycin and 3 μg PMBN to inhibit ECA biosynthesis was performed (Al-Dabbagh et al., 2008). DSP crosslinking showed WecG did not physically interact with any other protein and, unlike TagA, did not dimerise (Figure 6d). This supported the hypothesis that perhaps WecG is instead maintained to the membrane through lipid mediated interactions rather than a physical interaction with WzyE. Membrane fractionation of cells treated with tunicamycin to block ECA lipid-I production (Figure 7a) revealed that WecG could not be maintained exclusively at the membrane, and suggested that the biosynthetic intermediates themselves played a critical role in maintaining WecG's membrane

association. It is known that some glycosyltransferase's membrane association, such as MurM, are facilitated via direct interactions between the biosynthetic intermediate and the protein, where the biosynthetic intermediate becomes the tether facilitating membrane association (York et al., 2021).

To determine if WecG was maintained at the membrane with the aid of biosynthetic intermediates, chemical treatment of whole cells was performed in the PE860 *wecC* mutant. *wecC* mutants prevent the generation of ECA lipid-II (Figure 1) and it was showed that WecG remained associated with the membrane (Figure 7c) whereas, when cells were treated with tunicamycin it caused the dissociation of WecG from MFs (Figure 7a) which was similarly observed when expressing WecG from a *wecA* mutant strain (Figure 7b). These results suggest that WecG is indeed maintained to the membrane with aid of its biosynthetic, membrane-embedded substrate, ECA lipid-I. Overall, the results support the hypothesis that WecG is maintained to the membrane through interactions with ECA lipid-I, which is facilitated through its unusual, protruding CTD helices which are reminiscent GT-E-fold glycosyltransferases.

The GT-E fold is a novel glycosyltransferase family where unlike GT-A and GT-B folds, they contain a single Rossmann-fold domain followed by a series of three α-helices (O'Toole et al., 2021). The fold was first exhibited and described by Kattke et al. (2019), where they presented TagA as the first protein to be denoted with the novel fold. Despite the lack of an experimentally determined structure, WecG contains elements which are inconsistent with the biophysical definitions of GT-A, GT-B, GT-C, or GT-D-fold glycosyltransferases and, hence, due to WecG's similarities with TagA we characterize it as a GT-E-fold glycosyltransferase.

WecG lacks the canonical Asp-X-Asp motif which is used to coordinate Mg^{2+} or Mn^{2+}ions, where upon binding, induce local conformational changes which facilitate substrate binding and catalysis in GT-A class glycosyltransferases (Liang et al., 2015). Due to the relative length of WecG's peptide sequence, it is unlikely to form two Rossmann folds which are the characteristic of GT-B-fold glycosyltransferases where the binding pockets reside deep within the two Rossmann folds (Liang et al., 2015). Additionally, despite being an in silico generated structure, the structures predicted by I-TASSER, RaptorX, and Alphafold all independently predict that WecG consists of a single Rossmann fold, in which the remaining residues would be insufficient to fold into a second Rossmann fold (Figure 2a–c). GT-C glycosyltransferases commonly contain a N-terminal TM domain and a C-terminal globular domain. Common motifs of GT-C family glycosyltransferases are the WWDYG motif which is believed be to be the catalytic site of the glycosyltransferase with two additional, smaller motifs the DK (DXXK) and or MI (MXXI) motifs which are spatially adjacent to the WWDYG motif (Igura et al., 2008). Similar to the coordination motifs of GT-A family glycosyltransferases, WecG does not contain either of the three motifs and does not, indicated through the bioinformatic analysis, possess any TM segments; hence, it is improbable that WecG is a GT-C family glycosyltransferase. Lastly, GT-D-fold glycosyltransferases were first described by Zhang et al. (2014) with DUF1792 (PDB ID:4PFX) and are characterized by the presence of a DXE motif that facilitates Mn^{2+} ion binding which is required for catalysis. Like TagA, WecG shares limited predicted structural homology with DUF1792; however, this limited structural identity is most likely due to TagA being used as a structural template by I-TASSER and RaptorX during the in silico generation of the WecG structural model, and hence this limited similarity shared between DUF1792 and WecG is uncertain and speculative at best.

Due to the broad similarities between TagA and WecG, the GT-E family of glycosyltransferases best describe WecG. WecG, like TagA, possess a single in silico predicted, N-terminal Rossmann fold followed by three CTD α-helices which we have shown to be crucial to maintaining WecG's membrane association (Figure 4). Similarly to TagA, substitutions of conserved residues along CTD helix II of WecG prevent membrane association (Figure 5b,c) and, un-investigated in TagA, these CTD helix II substitutions were shown to greatly impact polysaccharide biosynthesis (Figure 5d). From these observations, it is clear that WecG is peripherally associated with the membrane via its CTD helices as is TagA. These similarities between TagA and the disparities between WecG and the structural requirements of the other GT fold families (A,B,C,D) place WecG as the second glycosyltransferase to be identified as a GT-E-fold glycosyltransferase.

In conclusion, this study reveals the true nature of WecG as a peripherally associated membrane protein and, in doing so, classifies WecG as a GT-E-fold glycosyltransferase. Additionally, the identification of WecG's reliance on its membrane association for ECA production provides new insight into our understanding of the biosynthesis of ECA, as well as provides novel drug targets to inhibit ECA biosynthesis.

CONFLICT OF INTEREST

The author(s) declare that there are no conflicts of interest.

ETHICS STATEMENT

The ECA and WzzE antibodies were produced under the National Health and Medical Research Council Australian Code of Practice for the Care and Use of Animals for Scientific Purposes and was approved by the University of Adelaide Animal Ethics Committee.

DATA AVAILABILITY STATEMENT

ORCID

Nicholas Maczuga https://orcid.org/0000-0001-7638-2613

REFERENCES

Al-Dabbagh, B., Mengin-Lecreulx, D. & Bouhss, A. (2008) Purification and characterization of the bacterial UDP-GlcNAc:undecaprenyl-phosphate GlcNAc-1-phosphate transferase WecA. *Journal of Bacteriology*, 190, 7141–7146.

Amar, A., Pezzoni, M., Pizarro, R.A. & Costa, C.S. (2018) New envelope stress factors involved in σ(E) activation and conditional lethality of *rpoE* mutations in *salmonella enterica*. *Microbiology*, 164, 1293–1307.

Baba, T., Ara, T., Hasegawa, M., Takai, Y., Okumura, Y., Baba, M. et al. (2006) Construction of *Escherichia coli* K-12 in-frame, single-gene knockout mutants: the Keio collection. *Molecular Systems Biology*, 2, 2006.0008.

Barr, K., Ward, S., Meier-Dieter, U., Mayer, H. & Rick, P.D. (1988) Characterization of an *Escherichia coli rff* mutant defective in transfer of N-acetylmannosaminuronic acid (ManNAcA) from UDP-ManNAcA to a lipid-linked intermediate involved in enterobacterial common antigen synthesis. *Journal of Bacteriology*, 170, 228–233.

Bottoms, C.A., Smith, P.E. & Tanner, J.J. (2002) A structurally conserved water molecule in Rossmann dinucleotide-binding domains. *Protein Science*, 11, 2125–2137.

Castelli, M.E. & Vescovi, E.G. (2011) The Rcs signal transduction pathway is triggered by enterobacterial common antigen structure alterations in *Serratia marcescens*. *Journal of Bacteriology*, 193, 63–74.

Danese, P.N., Oliver, G.R., Barr, K., Bowman, G.D., Rick, P.D. & Silhavy, T.J. (1998) Accumulation of the enterobacterial common antigen lipid II biosynthetic intermediate stimulates *degP* transcription in *Escherichia coli*. *Journal of Bacteriology*, 180, 5875–5884.

Datsenko, K.A. & Wanner, B.L. (2000) One-step inactivation of chromosomal genes in *Escherichia coli* K-12 using PCR products. *Proceedings of the National Academy of Sciences of the United States of America*, 97, 6640–6645.

Drozdetskiy, A., Cole, C., Procter, J. & Barton, G.J. (2015) JPred4: a protein secondary structure prediction server. *Nucleic Acids Research*, 43, W389–W394.

Eade, C.R., Wallen, T.W., Gates, C.E., Oliverio, C.L., Scarbrough, B.A., Reid, A.J. et al. (2021) Making the enterobacterial common antigen glycan and measuring its substrate sequestration. *ACS Chemical Biology*, 16(4), 691–700.

Gozdziewicz, T.K., Lukasiewicz, J. & Lugowski, C. (2015) The structure and significance of enterobacterial common antigen (ECA). *Postępy Higieny i Medycyny Doświadczalnej (Online)*, 69, 1003–1012.

Heifetz, A., Keenan, R.W. & Elbein, A.D. (1979) Mechanism of action of tunicamycin on the UDP-GlcNAc:dolichyl-phosphate GlcNAc-1-phosphate transferase. *Biochemistry*, 18, 2186–2192.

Igura, M., Maita, N., Kamishikiryo, J., Yamada, M., Obita, T., Maenaka, K. et al. (2008) Structure-guided identification of a new catalytic motif of oligosaccharyltransferase. *The EMBO Journal*, 27, 234–243.

Islam, S.T. & Lam, J.S. (2014) Synthesis of bacterial polysaccharides via the Wzx/Wzy-dependent pathway. *Canadian Journal of Microbiology*, 60, 697–716.

Jiang, X., Tan, W.B., Shrivastava, R., Seow, D.C.S., Chen, S.L., Guan, X.L. et al. (2020) Mutations in enterobacterial common antigen biosynthesis restore outer membrane barrier function in *Escherichia coli tol-pal* mutants. *Molecular Microbiology*, 2020(114), 991–1005.

Jorgenson, M.A., Kannan, S., Laubacher, M.E. & Young, K.D. (2016) Dead-end intermediates in the enterobacterial common antigen pathway induce morphological defects in *Escherichia coli* by competing for undecaprenyl phosphate. *Molecular Microbiology*, 100, 1–14.

Jumper, J., Evans, R., Pritzel, A., Green, T., Figurnov, M., Ronneberger, O. et al. (2021) Highly accurate protein structure prediction with AlphaFold. *Nature*, 596, 583–589.

Kajimura, J., Rahman, A. & Rick, P.D. (2005) Assembly of cyclic enterobacterial common antigen in *Escherichia coli* K-12. *Journal of Bacteriology*, 187, 6917–6927.

Källberg, M., Wang, H., Wang, S., Peng, J., Wang, Z., Lu, H. et al. (2012) Template-based protein structure modeling using the RaptorX web server. *Nature Protocols*, 7, 1511–1522.

Kattke, M.D., Gosschalk, J.E., Martinez, O.E., Kumar, G., Gale, R.T., Cascio, D. et al. (2019) Structure and mechanism of TagA, a novel membrane-associated glycosyltransferase that produces wall teichoic acids in pathogenic bacteria. *PLoS Pathogens*, 15, e1007723.

Krogh, A., Larsson, B., von Heijne, G. & Sonnhammer, E.L. (2001) Predicting transmembrane protein topology with a hidden Markov model: application to complete genomes. *Journal of Molecular Biology*, 305, 567–580.

Liang, D.M., Liu, J.H., Wu, H., Wang, B.B., Zhu, H.J. & Qiao, J.J. (2015) Glycosyltransferases: mechanisms and applications in natural product development. *Chemical Society Reviews*, 44, 8350–8374.

Lugtenberg, B., Meijers, J., Peters, R., van der Hoek, P. & van Alphen, L. (1975) Electrophoretic resolution of the 'major outer membrane protein' of *Escherichia coli* K12 into four bands. *FEBS Letters*, 58, 254–258.

Maciejewska, A., Kaszowska, M., Jachymek, W., Lugowski, C. & Lukasiewicz, J. (2020) Lipopolysaccharide-linked enterobacterial common antigen (ECA[LPS]) occurs in rough strains of *Escherichia coli* R1, R2, and R4. *International Journal of Molecular Sciences*, 21, 6038.

Maczuga, N.T., Tran, E.N.H. & Morona, R. (2022a) Topology of the *Shigella flexneri* enterobacterial common antigen polymerase WzyE. *Microbiology*, 168, 001183.

Maczuga, N., Tran, E.N.H., Qin, J. & Morona, R. (2022b) Interdependence of *Shigella flexneri* O antigen and enterobacterial common antigen biosynthetic pathways. *Journal of Bacteriology*, 204, e0054621.

Marolda, C.L., Tatar, L.D., Alaimo, C., Aebi, M. & Valvano, M.A. (2006) Interplay of the Wzx translocase and the corresponding polymerase and chain length regulator proteins in the translocation and periplasmic assembly of lipopolysaccharide o antigen. *Journal of Bacteriology*, 188, 5124–5135.

Meier-Dieter, U., Starman, R., Barr, K., Mayer, H. & Rick, P.D. (1990) Biosynthesis of enterobacterial common antigen in *Escherichia coli*. Biochemical characterization of Tn10 insertion mutants defective in enterobacterial common antigen synthesis. *The Journal of Biological Chemistry*, 265, 13490–13497.

Mestrom, L., Przypis, M., Kowalczykiewicz, P.A., Kumpf, M., Bento, I., Jarzębski, S. et al. (2019) Leloir glycosyltransferases in applied biocatalysis: a multidisciplinary approach. *International Journal of Molecular Sciences*, 20, 5263.

Mitchell, A.M., Srikumar, T. & Silhavy, T.J. (2018) Cyclic enterobacterial common antigen maintains the outer membrane permeability barrier of *Escherichia coli* in a manner controlled by YhdP. *mBio*, 9, e01321-18.

Murray, G.L., Attridge, S.R. & Morona, R. (2003) Regulation of *salmonella typhimurium* lipopolysaccharide O antigen chain length is required for virulence; identification of FepE as a second Wzz. *Molecular Microbiology*, 47, 1395–1406.

O'Toole, K.H., Imperiali, B. & Allen, K.N. (2021) Glycoconjugate pathway connections revealed by sequence similarity network analysis of the monotopic phosphoglycosyl transferases. *Proceedings of the National Academy of Sciences*, 118, e2018289118.

Purins, L., Van Den Bosch, L., Richardson, V. & Morona, R. (2008) Coiled-coil regions play a role in the function of the *Shigella flexneri* O-antigen chain length regulator WzzpHS2. *Microbiology*, 154, 1104–1116.

Ramos-Morales, F., Prieto, A.I., Beuzon, C.R., Holden, D.W. & Casadesus, J. (2003) Role for *Salmonella enterica* enterobacterial common antigen in bile resistance and virulence. *Journal of Bacteriology*, *185*, 5328–5332.

Saidijam, M., Azizpour, S. & Patching, S.G. (2018) Comprehensive analysis of the numbers, lengths and amino acid compositions of transmembrane helices in prokaryotic, eukaryotic and viral integral membrane proteins of high-resolution structure. *Journal of Biomolecular Structure & Dynamics*, *36*, 443–464.

Smith, S.M. (2017) Strategies for the purification of membrane proteins. *Methods in Molecular Biology*, *1485*, 389–400.

Swoboda, J.G., Campbell, J., Meredith, T.C. & Walker, S. (2010) Wall teichoic acid function, biosynthesis, and inhibition. *Chembiochem*, *11*, 35–45.

Takatsuki, A., Arima, K. & Tamura, G. (1971) Tunicamycin, a new antibiotic. I. Isolation and characterization of tunicamycin. *The Journal of Antibiotics*, *24*, 215–223.

Wang, R.F. & Kushner, S.R. (1991) Construction of versatile low-copy-number vectors for cloning, sequencing and gene expression in *Escherichia coli*. *Gene*, *100*, 195–199.

Waterhouse, A.M., Procter, J.B., Martin, D.M., Clamp, M. & Barton, G.J. (2009) Jalview version 2—a multiple sequence alignment editor and analysis workbench. *Bioinformatics*, *25*, 1189–1191.

Woodward, R., Yi, W., Li, L., Zhao, G., Eguchi, H., Sridhar, P.R. et al. (2010) In vitro bacterial polysaccharide biosynthesis: defining the functions of Wzy and Wzz. *Nature Chemical Biology*, *6*, 418–423.

Yang, J., Yan, R., Roy, A., Xu, D., Poisson, J. & Zhang, Y. (2015) The I-TASSER suite: protein structure and function prediction. *Nature Methods*, *12*, 7–8.

York, A., Lloyd, A.J., del Genio, C.I., Shearer, J., Hinxman, K.J., Fritz, K. et al. (2021) Structure-based modeling and dynamics of MurM, a *Streptococcus pneumoniae* penicillin resistance determinant present at the cytoplasmic membrane. *Structure*, *29*, 1–12.

Zhang, H., Zhu, F., Yang, T., Ding, L., Zhou, M., Li, J. et al. (2014) The highly conserved domain of unknown function 1792 has a distinct glycosyltransferase fold. *Nature Communications*, *5*, 4339.

SUPPORTING INFORMATION

Additional supporting information can be found online in the Supporting Information section at the end of this article.

How to cite this article: Maczuga, N., Tran, E. N. H. & Morona, R. (2022). Subcellular localization of the enterobacterial common antigen GT-E-like glycosyltransferase, WecG. *Molecular Microbiology, 118*, 403–416. https://doi.org/10.1111/mmi.14973